.

Supplementary Material

for "Conical-focusing: Mechanism for singular jetting from collapsing drop-impact craters"

by Tian, Yang & Thoroddsen

S0.1. *Numerical method*

The numerical simulations are conducted by the *Gerris* flow solver using the volume-of-fluid (VOF) method and extreme dynamic grid refinement to evolve the interface structure. *Gerris* is an open-source code solving the Navier-Stokes Equations with the quad/octree spatial adaptive mesh refinement (Popinet 2009). We perform axisymmetric simulations of the incompressible Navier-Stokes equations including a surface tension term in the momentum equations. Both fluids are incompressible. The computational domain $L^* \times L^*$ is shown in figure S1 where a spherical drop with a diameter $D^* = 0.2L^*$, density ρ_l^*, viscosity μ_l^* and surface tension σ^* falls with an inital velocity U_0 from a height $h^* = 0.05L^*$ under the gravitational acceleration g^*. The ambient gas has a density ρ_g^* and viscosity μ_g^*. The size of the domain is $L^* = 1$ and the depth of liquid pool is $0.6L^*$. The characteristic length, velocity and time are the drop diameter L^*, impact velocity U_i^* and L^*/U_i^*. Note that the impact velocity U_i^* varies for each impact. The left boundary is set as the symmetric axis. The right and bottom boundaries are no-slip conditions. The top boundary is open to the atmosphere. In simulations, only one Water/Glycerol mixture (μ_l = 7.3 cP, ρ_l = 1140 kg/m^3) is used. In order to compare with our experimental results, all impact parameters are set identical to the experimental ones.

The grid level is dynamically adapted based on the value of vorticity and the location next to the interface. Our mesh size is refined up to $2^{18} \times 2^{18}$ for simulations, which supplies a minimum grid size of ~ 70 nm. It has been demonstrated that *Gerris* is valid for simulating complex interfacial flows of similar complexity as herein, such as drop impact splashing and bubble bursting (Deike *et al.* 2018; Thoraval *et al.* 2012; Lai *et al.* 2018).

We use Level 12 for the initiation of the simulations, as in figure S1. When the simulation is close to the formation of the crater dimple, we gradually increase the grid level to the maximum, Level 18. Because *Gerris* uses an adaptive mesh refinement, the time step adjusts to finer increments as the grid size becomes smaller. The distribution of mesh cells along the interface of the air sheet at refinement level 18 is shown in figure S2. The cell concentration along the curved interface is usually high as the vorticity variation is large.

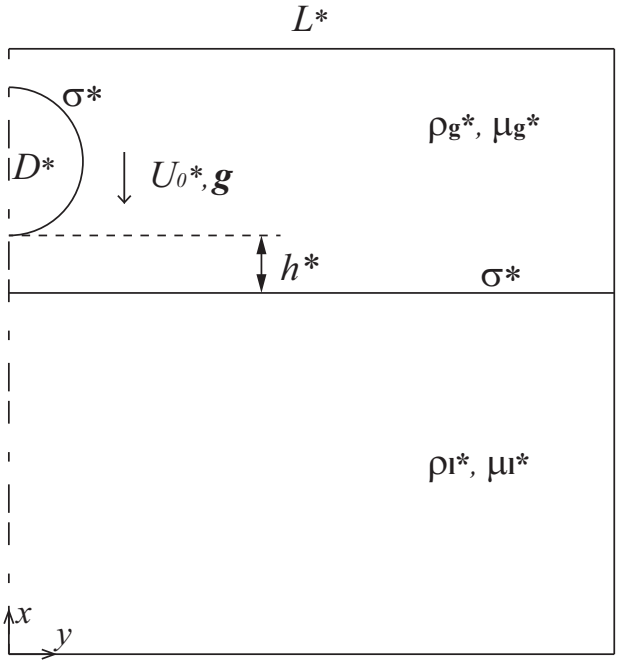

FIGURE S1. Sketch of the computational domain and settings of drop impact simulations.

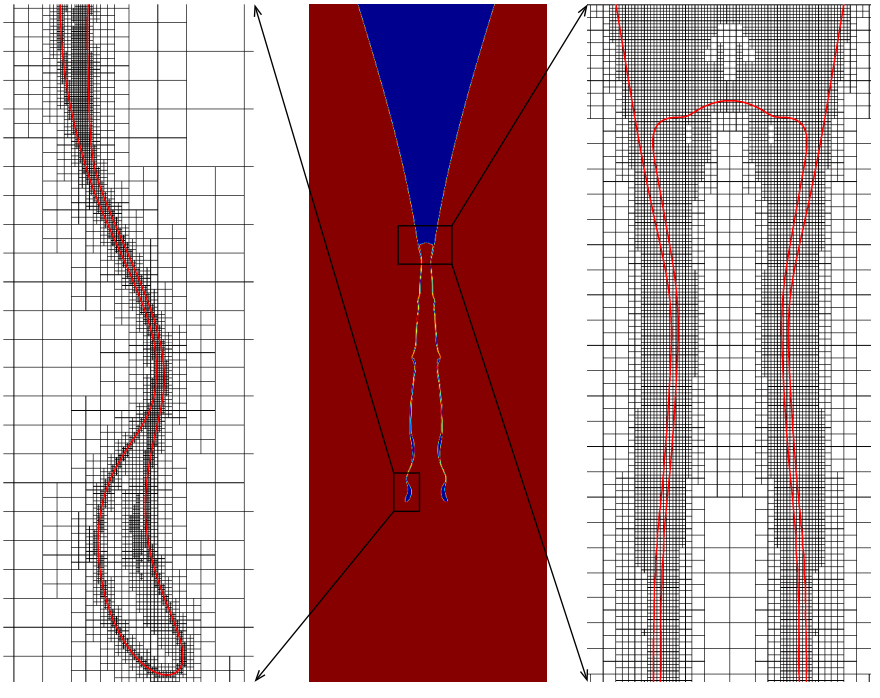

FIGURE S2. The distribution of mesh cells for the shedding case. The red line represents the air-liquid interface.

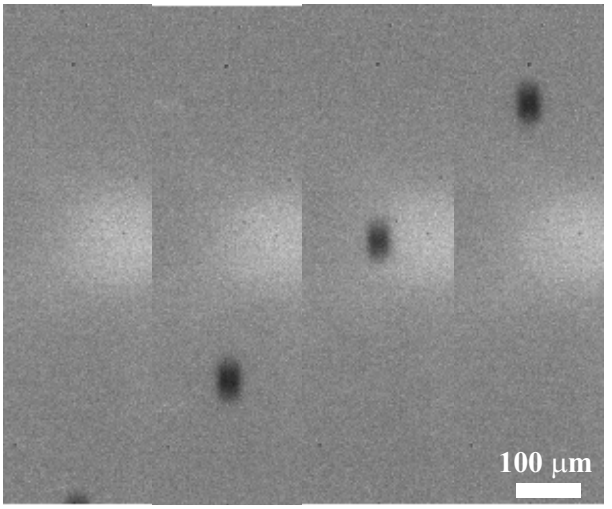

FIGURE S3. Frame sequence of a rising secondary droplet detached from jet tip. The camera frame rate is $0.4{\times}10^6$ fps, the droplet size is around 30 μm and the jet velocity is measured as $\simeq$ 40 m/s.

S0.2. *Jet velocity measurements*

The tips of the most singular jets break up into multiple secondary droplets following the jet formation and before they emerge out of the crater. The velocity of the first secondary droplet detached from the jet tip is therefore measured and counted as the jet velocity. By measuring the displacement and the corresponding frame time-interval from the high-speed video camera, the jet velocity can be easily obtained, as the jet velocity is almost constant during the short time, as shown in figure S3, for a typical case. The drop displacement is measured manually using the camera post-processing software (Phantom Camera Control, PCC 3.6) which allows us to keep the total measurement error below 3 pixels, for the fastest drops, which show the largest smearing in the images. Therefore, the uncertainty of the measured jet velocity is around $\pm$4 m/s, where the pixel resolution of the jet camera, at magnification of 8, is 3.5 μm/px. The uncertainty is smaller for slower droplet velocities, which show less image smearing.

REFERENCES

DEIKE, L., GHABACHE, E., LIGER-BELAIR, G., DAS, A. K., ZALESKI, S., POPINET, S. & SÉON, T. 2018 Dynamics of jets produced by bursting bubbles. *Phys. Rev. Fluids* **3** (1), 013603.

LAI, C. Y., EGGERS, J. & DEIKE, L. 2018 Bubble bursting: Universal cavity and jet profiles. *Phys. Rev. Lett.* **121** (14), 144501.

POPINET, S. 2009 An accurate adaptive solver for surface-tension-driven interfacial flows. *J. Comput. Phys.* **228** (16), 5838–5866.

THORAVAL, M.-J., TAKEHARA, K., ETOH, T. G., POPINET, S., RAY, P., JOSSERAND, C., ZALESKI, S. & THORODDSEN, S. T. 2012 von Kármán vortex street within an impacting drop. *Phys. Rev. Lett.* **108** (26), 264506.